Use of silane coupling agent for surface modification of zinc oxide as inorganic filler and preparation of poly(amide–imide)/zinc oxide nanocomposite containing phenylalanine moieties

SHADPOUR MALLAKPOUR[1,2,*] **and MARYAM MADANI**[1]

[1]Department of Chemistry, [2]Nanotechnology and Advanced Materials Institute, Isfahan University of Technology, Isfahan 84156-83111, I. R. Iran

Abstract. A series of novel poly(amide–imide)/ZnO nanocomposites with modified ZnO nanoparticles contents was prepared by ultrasonic irradiation. For this purpose, surface of ZnO nanoparticle was modified with γ-aminopropyltriethoxysilane as a coupling agent. Then the effect of surface modification on dispersion of nanoparticles, thermal stability and UV absorption property of the obtained nanocomposites were investigated. The resulting novel nanocomposites were characterized by several techniques. Field emission scanning electron microscopy and transmission electron microscopy analyses of the nanocomposites were performed in order to study the dispersion of nanofillers in the polymer matrix. According to thermogravimetry analysis results, the addition of ZnO nanoparticles improved thermal stability of the obtained nanocomposites. Since the resulting nanocomposites contain phenylalanine amino acid and ZnO, they are expected to be biocompatible as well as biodegradable.

Keywords. Poly(amide–imide); nanocomposite; coupling agent; γ-aminopropyltriethoxysilane; ZnO nanoparticles.

1. Introduction

Nanocomposites of nanoscale inorganic semiconductors and organic host polymers have attracted extensive interest due to a broad range of potential applications of these materials (Lu *et al* 2006; Li and Li 2010; Wang *et al* 2010). Among the semiconducting nanoparticles, zinc oxide (ZnO) is a II–VI group of semiconductor having wurtzite structure and a direct wide bandgap of 3·37 eV and a large exciton binding energy of 60 meV at room temperature (Wang *et al* 2008). ZnO is a versatile material that has been widely used in solar cells (Gal *et al* 2000), varistors (Shi *et al* 2003), bioimaging (Wu *et al* 2007) and piezoelectric devices (Wang 2009). Other applications include sunscreens (Vigneshwaran *et al* 2006), sensors (Corso *et al* 2008), antireflection coatings (Lu *et al* 2007) and antibacterial activity (Zhang *et al* 2007; Jin *et al* 2009). Incorporating ZnO nanoparticles into polymer matrices can modify its optical and mechanical properties due to a strong interfacial interaction between polymers and nanoparticles. Nanoparticle/polymer nanocomposites have been produced with different polymer matrices, such as polyimide (Hsu *et al* 2005), polystyrene (Chae and Kim 2005; Hong *et al* 2007; Tang *et al* 2007; Tang and Dong 2009), polyurethane (Zheng *et al* 2005) and poly(methylmethacrylate) (Ahmad *et al* 2007; Srivastava *et al* 2008). However, the inferior thermal stability of organic matrix may restrict the

composite's applications in electronic and optoelectronic industries.

Poly(amide–imide)s (PAI)s are well known thermally stable polymers and possess desirable characteristics, having the advantages of both polyamides and polyimides, such as good mechanical properties and easy processability (Mallakpour and Kowsari 2006; Mallakpour and Khani 2007; Mallakpour and Kolahdoozan 2007). These polymers are the best candidates as matrix for the preparation of polymeric nanocomposites. It is known that the properties of nanocomposites are significantly influenced by both the dispersing degree of nanoparticles in the base polymers and the interfacial interactions between the polymer and filler (Laachachi *et al* 2009). On the other hand, nanoparticles possess high surface energy, which may cause agglomeration of nanoparticles. To prevent the formation of agglomerated nanoparticles, the surface of nanoparticles must be modified with suitable coupling agent to ensure its perfect dispersion. Many studies have been done toward the organized fabrication of the surface of nanoparticles through organoalkoxysilane (Li *et al* 2005; Hong *et al* 2009; Mallakpour and Soltanian 2010).

Amino acids are multi functional materials that are biologically active and can be used for the synthesis of biodegradable polymers. These compounds attracted considerable interest due to their unique properties such as non toxic, high optical purity and low cost. The polymers with naturally occurring building blocks such as amino acids are expected to be biodegradable and biocompatible (Mallakpour *et al* 2010, 2011).

---

*Author for correspondence (mallak@cc.iut.ac.ir, mallak777@yahoo.com, mallakpour84@alumni.ufl.edu)

In the present study, surface modification of ZnO nanoparticles with γ-aminopropyltriethoxysilane coupling agent (KH550) was performed, and influence of ZnO on thermal stability and UV property of polymer were investigated. The optically active poly(amide–imide) (PAI) which was used as matrix for preparation of nanocomposites was prepared by polycondensation reaction of N,N'-(pyromellitoyl)-*bis*-phenylalanine diacid chloride **1** with 4,4′-diaminodiphenylsulfone **2**. Then the optically active PAI/ZnO nanocomposites were synthesized via ultrasonic irradiation process. The resulting novel nanocomposites were characterized by Fourier transform infrared spectroscopy (FT–IR), thermogravimetry analysis (TGA), X-ray diffraction (XRD), UV/vis spectroscopy, field emission scanning electron microscopy (FE–SEM) and transmission electron microscopy (TEM).

2. Experimental

2.1 *Materials*

Pyromellitic dianhydride (benzene-1,2,4,5-tetracarboxylic dianhydride) (from Merck Chemical Co., Germany) was used as received. 4,4′-diaminodiphenylsulfone **2** was used without further purification. N,N-dimethylacetamide (DMAc) was dried over BaO, then distilled in vacuum. *L*-Phenylalanine was used as obtained without further purification. The silane coupling agent, γ-aminopropyltriethoxy silane (KH550), was obtained from Merck Chemical Co. Nanosized ZnO powder was purchased from Neutrino Co. with an average particle size of 25–30 nm.

2.2 *Synthesis of polymer*

The monomer of N,N'-(pyromellitoyl)-*bis-L*-phenylalanine diacid chloride **1** was prepared by a procedure reported elsewhere (Mallakpour *et al* 2002). PAI **3** was synthesized by the polycondensation reaction of an equimolar mixture of diamine **2** with diacid chloride **1** in a DMAc/triethylamine (NEt₃) system (scheme 1) as reported in our previous study (Mallakpour and Dinari 2011).

2.3 *Preparation of PAI/ZnO nanocomposite*

At first nanoparticles were treated with silane coupling agent. The surface modification of ZnO nanoparticles was carried out as follows: firstly, the ZnO was dried at 110 °C for 24 h; secondly, 0·20 g of dried nano ZnO was sonicated for 15 min in absolute ethanol; thirdly, 0·03 mL coupling agent was added to this system and sonicated for 20 min; at last, the mixture was filtrated and dried at 60 °C for more than 24 h. For the preparation of nanocomposite (PAI/ZnO-KH550), PAI was dispersed in 20 mL of absolute ethanol, then different amounts of modified ZnO nanoparticles (4, 8 and 12 wt% of PAI), were mixed with suspension and irradiated under ultrasound waves for 4 h. The solvent was removed and the obtained solid was dried in vacuum at 80 °C for 2 h.
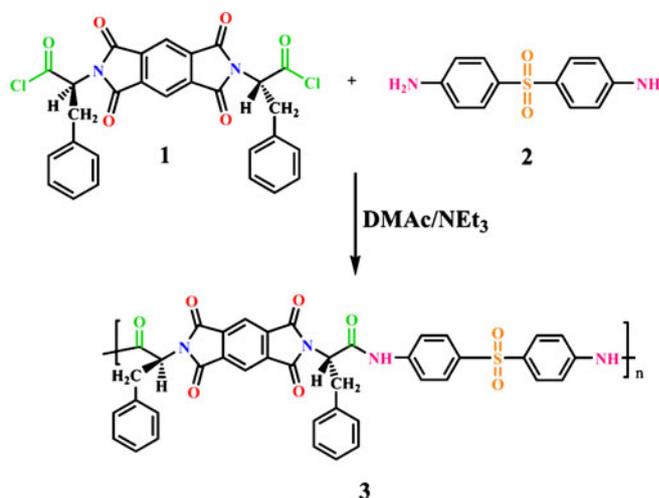
Scheme 1. Polycondensation reaction of monomer **1** with aromatic diamine **2**.

2.4 *Equipments*

A Jasco-680 Fourier transform infrared (FT–IR) spectroscope (Japan) was employed to examine the chemical bonds on the polymer and nanocomposites. Spectra of solids were obtained with KBr pellets. Vibration bands were reported as wavenumber (cm⁻¹). The band intensities are assigned as weak (w), medium (m), shoulder (sh), strong (s), and broad (br). Specific rotations were measured by a Jasco Polarimeter, Japan. Inherent viscosities were measured by a standard procedure using a Cannon-Fenske routine viscometer, Germany, at a concentration of 0·5 g/dL at 25 °C. Thermogravimetric analysis (TGA) was performed with a STA503 win TA at a heating rate of 10 °C/min from 25–800 °C under nitrogen. XRD pattern was acquired by using a Philips Xpert MPD X-ray diffractometer. The diffractograms were measured for 2θ, in the range of 10–100°, using Cu Kα incident beam ($\lambda = 1\cdot51418$Å). The dispersion morphology of the nanoparticles on PAI matrix was observed using field emission scanning electron microscopy [FE–SEM, HITACHI (S-4160)]. Transmission electron microscopy (TEM) images were obtained using a Philips CM 120 microscope with an accelerating voltage of 100 kV. UV/vis absorption of pure PAI and PAI/ZnO bionanocomposites measured in solid state samples by a UV/vis spectrometer, JASCO V-750, in the spectral range between 200 and 800 nm. The reaction occurred on a MISONIX ultrasonic liquid processor, XL-2000 SERIES, with a wave of frequency $2\cdot25 \times 10^4$ Hz and power, 100 W.

3. Results and discussion

3.1 *Fabrication of PAI/ZnO–KH550 nanocomposites*

PAI/ZnO–KH550 nanocomposites were fabricated by an ultrasonic irradiation technique. Cavitation or growth and
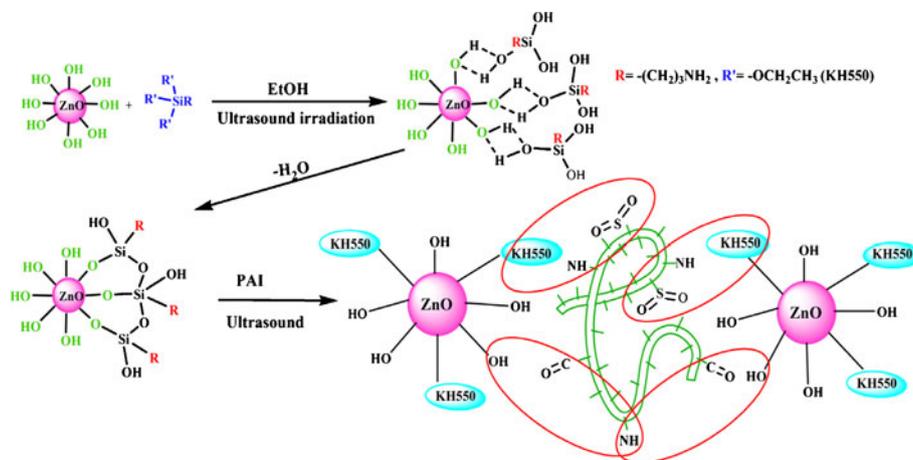
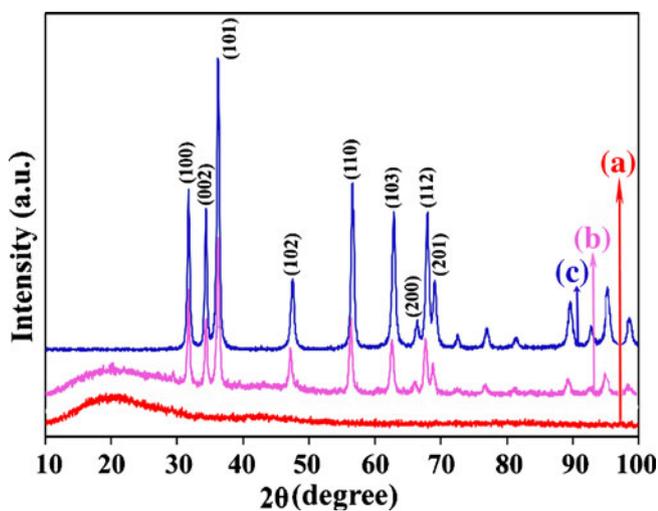**Scheme 2.** Schematic representation for preparation of PAI/ZnO nanocomposites.

Figure 1. XRD patterns of (**a**) PAI, (**b**) PAI/ZnO–KH550 (12 wt%) and (**c**) ZnO.

Figure 2. FT–IR spectra of ZnO nanoparticles and surface modified ZnO nanoparticles.

explosive disintegration of microscopic bubbles on a microsecond timescale occurs under ultrasonic irradiation. Ultrasonic irradiation can generate a rigorous environment of local temperature up to 5000 K and local pressure up to 500 atm. Therefore, ultrasound has been extensively applied in initiating polymerization, crushing, activation of materials, as well as in dispersion of nanoparticles in organic matrix (Kai *et al* 2005). In modification of nanoparticles, the hydroxyl group on the surface of ZnO will replace with OCH_2CH_3 of the KH550 to bond to it (Hong *et al* 2007; Tang *et al* 2007). In modified ZnO, the organic chains of KH550 can fulfil steric hindrance between inorganic nanoparticles and prevent their aggregation. As a result, the dispersion of nanoparticles in the polymer matrix increases with the decrease of surface energy of nanoparticles, which can be observed from the photographs of TEM and FE–SEM. The details of the fabrication mechanism are displayed in scheme 2.
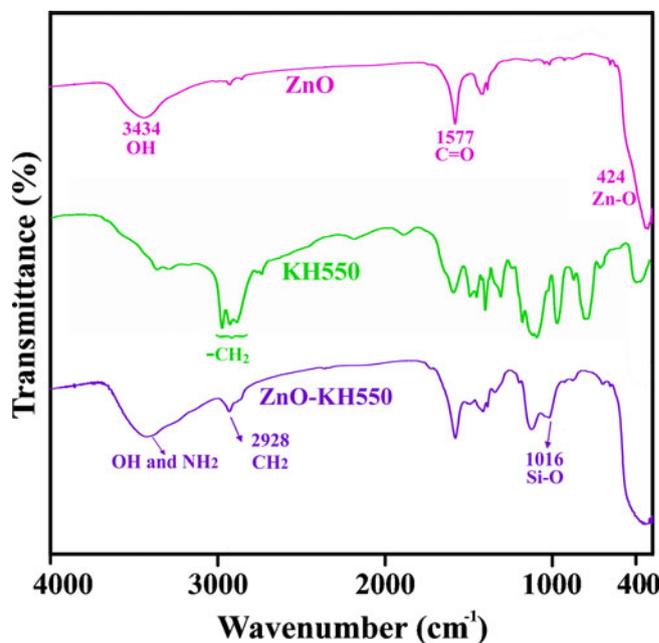
3.2 *X-ray diffraction data*

XRD patterns of PAI, PAI/ZnO–KH550 (12 wt%) and ZnO nanoparticles are shown in figure 1. Pure PAI was totally amorphous in nature, which did not show any sharp diffraction peaks. Figure 1(b) shows XRD pattern of nanocomposite with 12 wt% of ZnO–KH550, indicating that the morphology of ZnO nanoparticles has not been changed during the process. In figure 1(c), a series of characteristic peaks: (100), (002), (101), (102), (110), (103), (200), (112) and (201) are noticed, which are in accordance with the zincite phase of ZnO (International Centre for diffraction data, JCPDS 5-0664). The average crystallite size, D, was calculated by the Debye–Scherrer formula

$$(D = K\lambda/\beta \cos\theta),$$

where K is the Scherrer constant, λ the X-ray wavelength, β the peak width at half-maximum, and θ the Bragg diffraction angle. From the Debye–Scherrer formula, we obtained the crystallite diameter as 24–37 nm for ZnO–KH550 in polymer matrix.
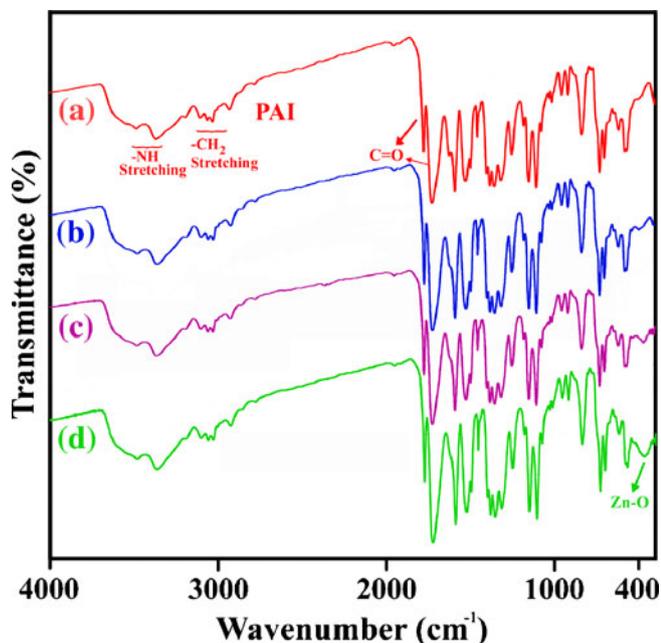

Figure 3. FT–IR spectra of PAI/ZnO–KH550 nanocomposites: (**a**) pure PAI, (**b**) PAI/ZnO (4 wt%), (**c**) PAI/ZnO (8 wt%) and (**d**) PAI/ZnO (12 wt%).

3.3 *FT–IR spectra*

Figure 2 shows typical FT–IR spectra of pure ZnO nanoparticles, KH550 coupling agent and modified ZnO nanoparticles. FT–IR spectrum of ZnO nanoparticles showed broad peak at 3434 cm^{-1} due to the stretching vibrations of the –OH group on the surface of ZnO nanoparticles, the peak at 1577 cm^{-1} resulting from residual acetate groups of zinc acetate which was used for the synthesis of ZnO nanoparticles and a high intensity broad band around 424 cm^{-1} due to the vibration mode of zinc and oxygen bond. FT–IR spectrum of functionalized ZnO with KH550 in comparison of KH550 coupling agent gave a broad absorption band located at 3419 cm^{-1}, which is attributed to –OH and –NH$_2$ groups. The peaks at 2928 and 1016 cm^{-1} can be assigned to the symmetric methylene stretch (–CH$_2$), and the Si–O stretch, respectively. FT–IR indicated that coupling agents have been successfully grafted onto the surface of ZnO nanoparticles.

FT–IR spectra of the polymer and nanocomposites are shown in figure 3. The spectrum of PAI showed absorptions around 3360 cm^{-1} (N–H), two overlapped carbonyl (amide and imide's C=O) absorptions at 1776, 1725 and 1663 cm^{-1}, respectively. Absorptions at 1380 and 727 cm^{-1} indicate the presence of imide heterocycle in the polymer structure. Absorptions at 1251 and 1150 cm^{-1} are due to the sulfone moiety (SO$_2$ stretching). The spectra of the nanocomposites with different ZnO–KH550 contents (figures 3b–d) exhibit the characteristic absorption peaks corresponding to polymeric groups and nanoparticles. The incorporation of ZnO nanoparticles in PAI caused slight changes in the intensities
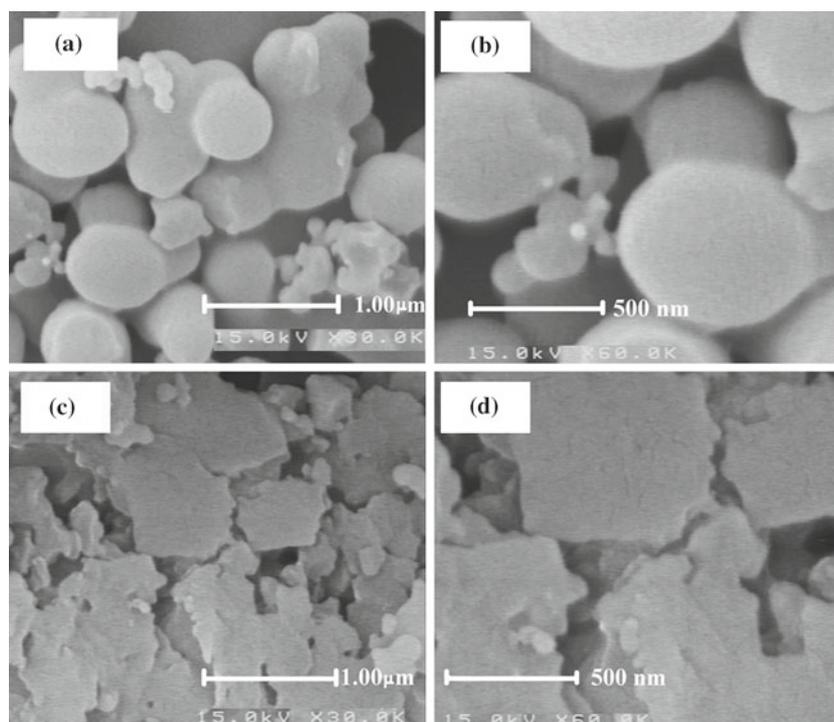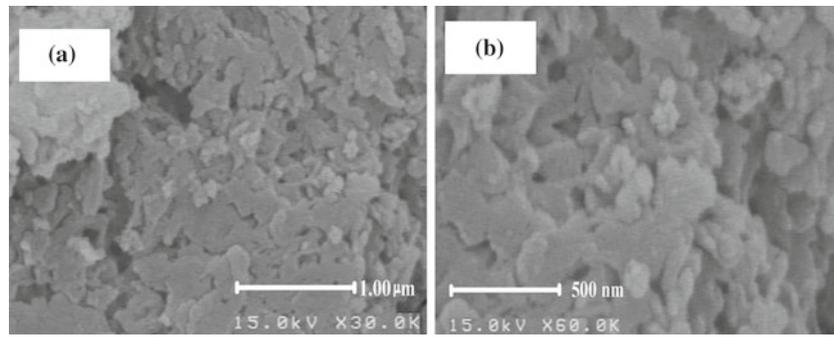

Figure 4. FE–SEM micrographs of pure PAI.

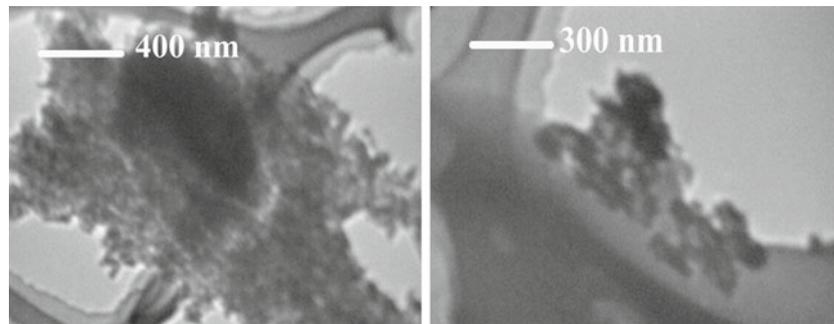**Figure 5.** FE–SEM images of PAI/ZnO (12 wt%) with different magnifications.

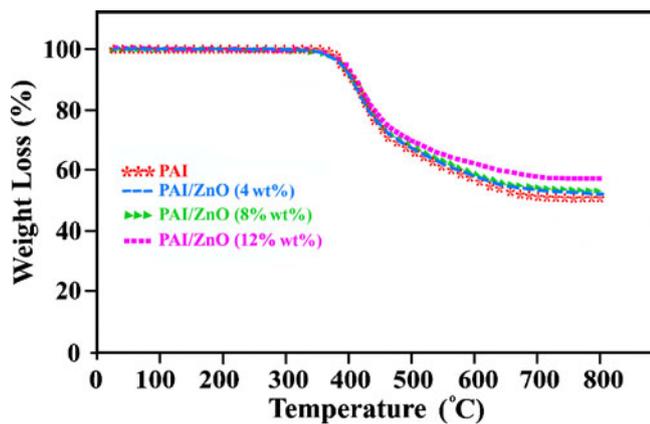
Figure 6. TEM micrograph of PAI/ZnO (12 wt%).

Figure 7. TGA thermograms of pure PAI and PAI/ZnO nanocomposites with different nanofiller contents.

of absorption bands as well as the formation of new absorption bands in the range of 600–400 cm^{-1} which is attributed to the Zn–O stretching. This result confirmed the existence of ZnO nanoparticles in PAI matrix.

3.4 *Effect of coupling agent on dispersion of ZnO nanoparticles*

Figure 4 shows FE–SEM of PAI with different magnifications. It indicates that the morphology of pure PAI has spherical-shaped spheres.

The morphology of nanocomposite was revealed by FE–SEM (figure 5). From these images, it was found that the surface modified ZnO nanoparticles with coupling agent are quasi-spherical in shape. The results showed that the ZnO nanoparticles were homogeneously dispersed in PAI matrix and their average particle size was below 60 nm.

Figure 6 shows representative TEM micrographs of PAI/ZnO–KH550 (12 wt%) nanocomposite. The micrographs confirmed that the ZnO–KH550 particles were well dispersed in the polymer matrix having a diameter size from 30 nm to 50 nm. This result is in accordance with the value calculated from X-ray diffraction. The obtained results indicate that the effect of coupling agent plays an important

Table 1. Thermal properties of PAI and PAI/ZnO–KH550 nanocomposites.

Sample code	T_5 (°C)[a]	T_{10} (°C)[b]	Char yield (%)[c]
PAI	383	410	50·0
PAI/ZnO–KH550 (4 wt%)	388	412	52·5
PAI/ZnO–KH550 (8 wt%)	390	410	53·2
PAI/ZnO–KH550 (12 wt%)	393	413	57·5

[a]Temperature at which 5% weight loss was recorded by TGA at a heating rate of 10 °C/min under a nitrogen atmosphere. [b]Temperature at which 10% weight loss was recorded by TGA at a heating rate of 10 °C/min under a nitrogen atmosphere, [c]weight percentage of material left undecomposed after TGA analysis at a temperature of 800 °C under nitrogen atmosphere.
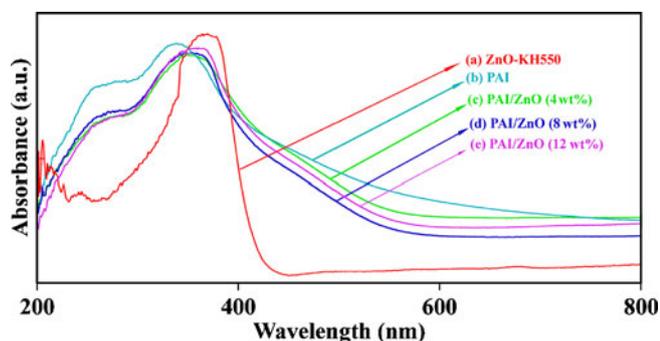
Figure 8. UV/vis absorption spectra of ZnO–KH550, PAI and PAI/ZnO nanocomposites.

role in dispersion of the nanoparticles. For coupling agent KH550, functional group that provides the interaction with PAI matrix is the amino group that can interact with the amide group (C=O), S=O and –NH of PAI via hydrogen bonding.

3.5 *Thermal analysis*

Figure 7 shows TGA curves of PAI/ZnO–KH550 with different ZnO contents. All nanocomposites demonstrate one-step decomposition. It is clear that the samples exhibit a very good thermal stability before 300 °C and decompose around 350–400 °C in N_2 atmosphere, which was further improved when ZnO was introduced. The char yields at 800 °C of the nanocomposites with different ZnO contents are higher than that of pure PAI; this increase in thermal stability may be a result from the high thermal stability of the ZnO nanoparticles. In addition, ZnO is a nanoscale particle, which offers a larger surface area and improves the effect of thermal cover. (TGA data are summarized in table 1).

3.6 *UV/vis absorption*

UV/vis absorption of ZnO–KH550, PAI/ZnO–KH550 nanocomposites and PAI are shown in figure 8. The maximum absorption peak of pure PAI is shown to be around 338 nm and PAI displays absorbance in the UV region due to its delocalized π-electrons. The ZnO–KH550 shows UV absorption peak maximum at 368 nm. For the PAI/ZnO nanocomposites, red shift occurred to some extent up to 360 nm in comparison with pure PAI. The UV shielding ability relates with the scattering and/or absorbance of nanoparticles. The scattering property plays an important role in shielding of UV irradiation. The range of UV wavelengths is often subdivided into UV–A (380–315 nm), UV–B (315–280 nm), and UV–C (280–10 nm). Thus, the resulting nanocomposites can be applied to block the UV–A radiation.

4. Conclusions

PAI/ZnO–KH550 nanocomposites were synthesized through ultrasonic irradiation technique. Under ultrasonic condition,

the modified nanoparticles could be dispersed uniformly and will combine with PAI via the amino groups of coupling agent and different interactions with the functional groups of the polymer. Modified nanoparticles will combine with PAI via the hydrogen bonding of NH_2 coupling agent with –NH, C=O and –SO_2 groups in PAI. Also, the unmodified –OH groups on the surface of ZnO nanoparticles can interact with the C=O and NH groups of PAI chain through hydrogen bonding. The result of FE–SEM and TEM prove that functionalized ZnO showed a fine dispersion in polymeric matrix. TGA results indicated that the incorporation of ZnO nanoparticles can improve thermal stability of the nanocomposites. UV/vis absorption spectra of the prepared nanocomposites were red shifted in comparison with pure PAI. These nanocomposite materials have the potential to be used as UV absorbance in the design of optical coatings (Mandal *et al* 2009; Sinha *et al* 2011). The PAI was chosen as polymeric matrix for the preparation of nanocomposite which is optically active and biodegradable due to the existence of phenylalanine amino acid in its backbone. On the other hand, the ZnO nanoparticle is environmentally friendly, therefore, having both natural amino acid and ZnO nanoparticles in these nanocomposites are expected to have biodegradability properties.

References

Ahmad S, Ahmad S and Agnihotry S A 2007 *Bull. Mater. Sci*. **30** 31
Chae D W and Kim B C 2005 *Polym. Adv. Technol*. **16** 846
Corso C D, Dickherber A and Hunt W D 2008 *Biosens. Bioelectron*. **24** 805
Gal D, Hodes G, Lincot D and Schock H W 2000 *Thin Solid Films* **361–362** 79
Hong R Y, Chen L L, Li J H, Li H Z, Zheng Y and Ding J 2007 *Polym. Adv. Technol*. **18** 901
Hong R Y, Li J H, Chen L L, Liu D Q, Li H Z, Zheng Y and Ding J 2009 *Powder Technol*. **189** 426
Hsu S C, Whang W T, Hung C H, Chiang P C and Hsiao Y N 2005 *Macromol. Chem. Phys*. **206** 291
Jin T, Sun D, Su J Y, Zhang H and Sue H J 2009 *J. Food. Sci*. **74** 46
Kai Z, Qiang F, Yuhong H and Dehui Z 2005 *Sci. China. Ser. B. Chem*. **48** 545
Laachachi A, Ruch D, Addiego F, Ferriol M, Cochez M and Cuesta J M L 2009 *Polym. Degrad. Stabil*. **94** 670
Li H, You B, Gu G, Wu L and Chen G 2005 *Polym. Int*. **54** 191
Li S C and Li Y N 2010 *J. Appl. Polym. Sci*. **116** 2965

Lu H, Xu X, Li X and Zhang Z 2006 *Bull. Mater. Sci.* **29** 485

Lu N, Lu X, Jin X and Lu C 2007 *Polym. Int.* **56** 138

Mallakpour S and Dinari M 2011 *Polymer* **52** 2514

Mallakpour S and Kowsari E 2006 *Polym. Bull.* **57** 169

Mallakpour S and Khani M 2007 *Polym. Bull.* **59** 587

Mallakpour S and Kolahdoozan M 2007 *J. Appl. Polym. Sci.* **104** 1248

Mallakpour S and Soltanian S 2010 *Polymer* **51** 5369

Mallakpour S E, Hajipour A R and Habibi S 2002 *J. Appl. Polym. Sci.* **86** 2211

Mallakpour S, Tirgir F and Sabzalian M R 2010 *J. Polym. Environ.* **18** 685

Mallakpour S, Tirgir F and Sabzalian M R 2011 *J. Polym. Res.* **18** 373

Mandal S K, Nath T K and Manna I 2009 *Nanosci. Nanotech. Lett.* **1** 99

Shi J, Cao Q, Wei Y and Huang Y 2003 *Mater. Sci. Eng.* **B99** 344

Sinha S K, Bhattacharya R, Ray S K and Manna I 2011 *Mater. Lett.* **65** 146

Srivastava S, Haridas M and Basu J K 2008 *Bull. Mater. Sci.* **31** 213

Tang E and Dong S 2009 *Colloid. Polym. Sci.* **287** 1025

Tang E, Liu H, Sun L, Zheng E and Cheng G 2007 *Eur. Polym. J.* **43** 4210

Vigneshwaran N, Kumar S, Kathe A A, Varadarajan P V and Prasad V 2006 *Nanotechnology* **17** 5087

Wang J, Zhang S, You J, Yan H, Li Z, Jing X and Zhang M 2008 *Bull. Mater. Sci.* **31** 597

Wang J, Tsuzuki T, Tang B, Cizek P, Sun L and Wang X 2010 *Colloid Polym. Sci.* **288** 1705

Wang Z L 2009 *Chinese Sci. Bull.* **54** 4021

Wu Y L, Lim C S, Fu S, Tok A I Y, Lau H M, Boey F Y C and Zeng X T 2007 *Nanotechnology* **18** 215604

Zhang L, Jiang Y, Ding Y, Povey M and York D 2007 *J. Nanopart. Res.* **9** 479

Zheng J, Ozisik R and Siegel R W 2005 *Polymer* **46** 10873